

## Electrogenerative leaching for sphalerite-MnO<sub>2</sub> in the presence of *Acidithiobacillus thiooxidans*

WANG Shao-fen(王少芬)<sup>1</sup>, XIAO Li(肖利)<sup>2,3</sup>, FANG Zheng(方正)<sup>2</sup>,  
QIU Guan-zhou(邱冠周)<sup>2</sup>, WANG Chun-xiong(王春雄)<sup>3</sup>

1. College of Chemistry and Biological Engineering, Changsha University of Science and Technology, Changsha 410004, China;
2. School of Resources Processing and Bioengineering, Central South University, Changsha 410083, China;
3. Metallurgic Engineering College, Hunan Industrial University, Zhuzhou 412000, China

Received 6 July 2009; accepted 30 December 2009

**Abstract:** A dual cell system was used to study the electrogenerative leaching sphalerite-MnO<sub>2</sub> in the presence and absence of *Acidithiobacillus thiooxidans* (*A. thiooxidans*). The polarization of anode and cathode, and the relationship between the electric quantity ( $Q$ ) and some factors, such as the dissolved rate of Zn<sup>2+</sup> and Fe<sup>2+</sup>, and the time in the bio-electro-generating simultaneous leaching (BEG) and electro-generating simultaneous leaching (EGL) were studied. A three-electrode system was applied to studying anodic and cathodic self-corrosion current, which was inappreciable compared with the galvanic current between sphalerite and MnO<sub>2</sub>. The results show that the dissolved Zn<sup>2+</sup> in the presence of *A. thiooxidans* is nearly 43% higher than that in the absence of *A. thiooxidans*; the electrogenerative quantity in the former is about 150% more than that in the latter. The accumulated sulfur on the surface of sulfides produced in the electrogenerative leaching process can be oxidized in the presence of *A. thiooxidans*, and the ratio of biologic electric quantity reaches 27.9% in 72 h.

**Key words:** *A. thiooxidans*; electrogenerative leaching; sphalerite

### 1 Introduction

The electro-generating leaching (EGL)[1–3] has been applied to sulfide minerals. In the process, the Gibbs free energy is transformed to an applicable electrical work and the leaching products are acquired simultaneously. In EGL, a galvanic cell with anolyte and catholyte compartments separated by an anion membrane which allows anions to migrate freely is designed[4–8]. The compact sulfide powder and MnO<sub>2</sub> powder are used as anode and cathode, respectively. The new technique can not only simplify purification of leached solution, but also produce element sulfur instead of gaseous H<sub>2</sub>S [9] and SO<sub>2</sub>[10] which pollute environment in traditional leaching.

There are some reports on hydrometallurgical treatment of sphalerite[4, 11–16], including EGL of sphalerite-MnO<sub>2</sub>[4, 11]. XIAO et al[11] pointed out that

the surface of leached sulfides covered by the accumulated sulfur hinders the anodic reaction to continue, greatly reducing the output of electric energy in EGL. The rates of interaction of the two minerals were much higher than their self-corrosion rates [12–13]. It is also shown[14] that the sulfur film covered on the mineral surface passivates the anode. TAKAMI [15] presented that the elemental sulfur could be removed by the *Acidithiobacillus thiooxidans* (*A. thiooxidans*) in simultaneous leaching of ZnS-MnO<sub>2</sub>.

*A. thiooxidans* plays an important role in the biochemical treatment of sulfur[16]. The bacteria can obtain energy from oxidation of sulfur substrate and make the sulfur covered on surface of minerals be oxidized and removed. However, few works on leaching of sphalerite in the presence of *A. thiooxidans* are reported, especially the mechanism of bio-oxidization for the mineral is still indistinct.

In this study, to explore the mechanism of BEGL for

sphalerite in the presence of *A. thiooxidans*, the relations between time and such data as the electric quantity and the dissolved rate of  $Zn^{2+}$  and  $Fe^{2+}$  in a galvanic cell with *A. thiooxidans* were analyzed, and the evidence of SEM for oxidation remains of the mineral was studied.

## 2 Experimental

### 2.1 Minerals

The selected sphalerite was a natural hand-sorted ores from a domestic mine. Its element analysis is listed in Table 1.

**Table 1** Chemical composition of sphalerite (mass fraction, %)

Zn	S	Fe	Sn	Si
51.54	29.74	12.27	0.33	4.45

The XRD analysis shows that ZnS and FeS coexist in the minerals.

### 2.2 Set and electrode for EGL

The set used was an electrolysis cell made of PVC, which divided into anode and cathode compartments of 200 mL capacity connected by an anion membrane [4-5].

The electrodes made of powders of sphalerite and  $MnO_2$ , respectively. The sphalerite-acetylene black paste and  $MnO_2$ -acetylene black paste were compacted in an acid-resisting nylon filter net with aperture size of 45  $\mu m$ , respectively. Two carbon rods with diameter of 2.48 cm were separately connected to the two mixtures to gather electric current respectively. Air-blowing tubes were separately inserted into anolyte and catholyte rooms to agitate and to supply oxygen for bacteria. The pH value, electrode potentials (vs SCE) and output voltage of the cell were measured with a PHS-3C digital acidometer, the output current with an amperemeter and the concentration of oxygen with a Degussa oxygen meter. All of the measured instruments were calibrated before each run.

### 2.3 Solutions and bacteria

The solutions were prepared using AR reagents and distilled water. The molarities of the bacteria culture medium were: 22.7 mmol/L  $(NH_4)_2SO_4$ , 1.34 mmol/L KCl, 2.87 mmol/L  $K_2HPO_4$ , 2.03 mmol/L  $MgSO_4 \cdot 7H_2O$  and  $6.09 \times 10^{-2}$  mmol/L  $Ca(NO_3)_2$ . To compare, the medium was acidified first to pH 1.8 using  $H_2SO_4$  as anolyte of EGL, and the same nutrient medium with exponential growth phase bacteria was as anolyte of BEGL. The molarity of oxygen in the solution was 0.184 mmol/L. A pure strain of *A. thiooxidans* that could breed

on sphalerite was from Hubei Province of China.

### 2.4 Self-corrosion measurements

A three-electrode system with a working electrode of  $MnO_2$  or sphalerite-acetylene black paste, a platinum counter and a saturated calomel electrode (SCE) reference were used for self-corrosion measurements. Polarization was measured with the scanning rate of 0.1 mV/s by the CHI660B electrochemical workstation with a computer. All potentials presented in this work were against SCE.

## 3 Results and discussion

### 3.1 Anodic and cathodic polarizability in EGL and BEGL

The Evans diagram, anodic and cathodic polarization, and interior resistance of the cell were used to study the control factor in EGL and BEGL processes. Generally, the bigger the value of resistance is, the greater the effect on the leaching reaction[4]. Fig.1 shows the Evans diagram of EGL and BEGL for sphalerite- $MnO_2$ .

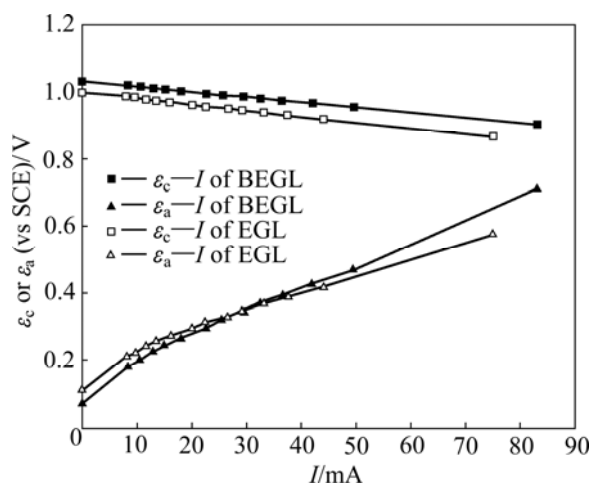


**Fig.1** Evans diagram of BEGL and EGL for sphalerite- $MnO_2$

As it can be seen from Fig.1, the currents increase with the increase of over-potential of cathode ( $\eta_c$ ) and the over-potential of anode ( $\eta_a$ ). Polarization is defined as:

$$P = \frac{d\varepsilon}{dI} = \frac{\eta}{I} \quad (1)$$

where  $\eta$  is the over-potentials, and  $I$  is the galvanic current.

The polarizations of anode and cathode are  $P_a$  and  $P_c$ , respectively:

$$P_a = \frac{\eta_a}{I} \quad (2)$$

$$P_c = \frac{\eta_c}{I} \quad (3)$$

$$\varepsilon_c - \varepsilon_a = \eta_c + \eta_a + IR = IP_c + IP_a + IR \quad (4)$$

$$I = \frac{\varepsilon_c - \varepsilon_a}{P_c + P_a + R} \quad (5)$$

where  $R$  is the interior resistance of the system.  $P_a$ ,  $P_c$ ,  $R$ , and  $J$  (density of current) are listed in Table 2. The over-potentials of anode and cathode increase with the decrease of galvanic voltage in 36 h during EGL and BEGL processes.

It is seen from Table 2 that the  $P_a$  and  $R$  are smaller at first due to the electric catalytic activity of acetylene black. Another important feature of polarization reflects to the data of different stages (see Table 2). Compared with EGL, the polarization  $P_a$  comes to steady-value about 20  $\Omega$  with the decrease of the galvanic current in BEGL system as the process is going on. This could be attributed to the fact that elemental sulfur accumulated on the electrode inhibits the progress of the EGL, while be oxidized by oxygen with the promotion of *A. thiooxidans* in BEGL. The decrease in acidity of the solution in both processes might be the reason for the increase in polarization  $P_c$ .

**Table 2**  $P_c$ ,  $P_a$ ,  $R$  and  $J$  of EGL and BEGL for sphalerite-MnO<sub>2</sub>

Process	Time/h	$P_c/\Omega$	$P_a/\Omega$	$R/\Omega$	$J/(\text{mA}\cdot\text{cm}^{-2})$
BEGL	0	1.93	6.8	1.98	8.72
	12	6.37	17.56	2.94	7.93
	24	7.85	19.43	3.47	7.88
	36	14.63	20.93	3.29	7.37
EGL	0	1.54	8.04	1.21	10.25
	12	5.46	22.51	2.92	5.53
	24	7.84	28.63	2.63	4.86
	36	15.47	35.17	2.45	3.73

### 3.2 Self-corrosion for sphalerite and MnO<sub>2</sub> electrodes

In addition to the galvanic current in EGL and BEGL system, there also exists the self-corrosion in two electrodes, respectively. Comparison of the galvanic current and the self-corrosion current could estimate which one is predominant. A convenient way to determine the self-corrosion is to plot Tafel curves of the individual half-cells. The Tafel curves of sphalerite anode with or without *A. thiooxidans* and MnO<sub>2</sub> cathode in 1 mol/L H<sub>2</sub>SO<sub>4</sub> are shown in Fig.2.  $E_{\text{corr}}$ ,  $J_{\text{corr}}$ , and  $R_p$  obtained from the Tafel curves are listed in Table 3.

For sphalerite, the self-corrosion current ( $J_{\text{corr}}$ ) as seen from Table 3 is negligible compared with the

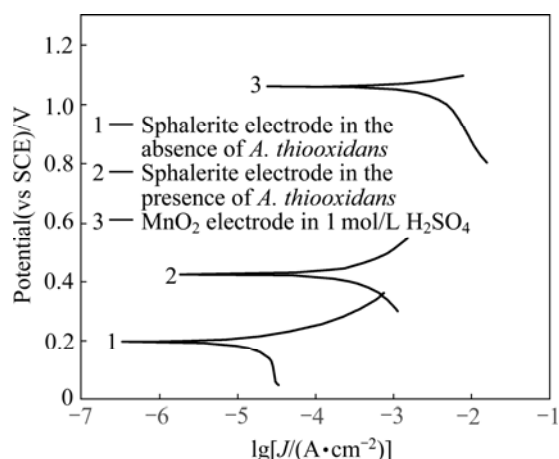


**Fig.2** Tafel curves

**Table 3**  $E_{\text{corr}}$ ,  $J_{\text{corr}}$  and  $R_p$  calculated from Tafel curves

Electrode	$E_{\text{corr}}(\text{vs SCE})/\text{V}$	$J_{\text{corr}}/(\text{mA}\cdot\text{cm}^{-2})$	$R_p/\Omega$
Sphalerite (with <i>A. thiooxidans</i> )	0.425	0.097 0	92
Sphalerite (germfree)	0.197	0.008 7	1 034
MnO <sub>2</sub>	1.062	1.120 0	17

galvanic current density ( $J$ ) shown in Table 2. For MnO<sub>2</sub>, the self-corrosion current is almost the same magnitude as the galvanic current. Accordingly, the galvanic interaction for sphalerite predominates over their individual self-corrosion whether in EGL or BEGL processes.

### 3.3 Electric quantity and leaching ratio in EGL and BEGL processes

Assume that the all-transferred charge is due to S<sup>2-</sup> to S<sup>0</sup> and is considered the theoretic electric quantity ( $Q_t$ ), which can be calculated by the Faraday's law. However, the measured electric quantity ( $Q_m$ ) in BEGL process is larger than the theoretic one. This means that the transferred charge is not only S<sup>2-</sup> to S<sup>0</sup> but also part of S<sup>0</sup> to sulfate group that is called as biologic electric quantity ( $Q_b$ ). The biologic electric quantity is defined as the difference between the measured and the theoretic one. The ratio of biologic electric quantity to the measured electric quantity can be used to predict the progress of BEGL process.

Table 4 shows the relationship between time and such factors as the dissolved rate of Zn<sup>2+</sup> and Fe<sup>2+</sup>,  $Q_t$  and  $Q_m$  in EGL process.

Table 5 gives the relationship between time and such factors as the dissolved rate of Zn<sup>2+</sup> and Fe<sup>2+</sup>, the biologic electric quantity ( $Q_b$ ) and ratio of biologic electric quantity to the measured one (ratio of  $Q_b$ ) in BEGL process.

**Table 4** Relationship between time and such factors as dissolved rates of  $Zn^{2+}$ ,  $Fe^{2+}$ ,  $Q_t$  and  $Q_m$  in EGL process

Time/h	Dissolved rate/%		$Q_t/C$	$Q_m/C$
	$Zn^{2+}$	$Fe^{2+}$		
12	22.21	32.56	975.96	976.35
24	32.54	49.54	1445.73	1451.55
36	39.02	58.02	1722.03	1667.55

**Table 5** Relationship between time and dissolved rates of  $Zn^{2+}$ ,  $Fe^{2+}$ ,  $Q_b$  and ratio of  $Q_b$  in BEGL process

Time/h	Dissolved rate/%		$Q_b/C$	Ratio of $Q_b/\%$
	$Zn^{2+}$	$Fe^{2+}$		
12	30.21	36.96	109.11	7.93
24	47.41	49.86	558.51	22.55
36	56.12	61.09	854.71	27.19
48	63.45	72.24	1 007.35	27.81
60	69.71	79.65	1 093.68	27.57
72	72.16	87.13	1 167.29	27.90

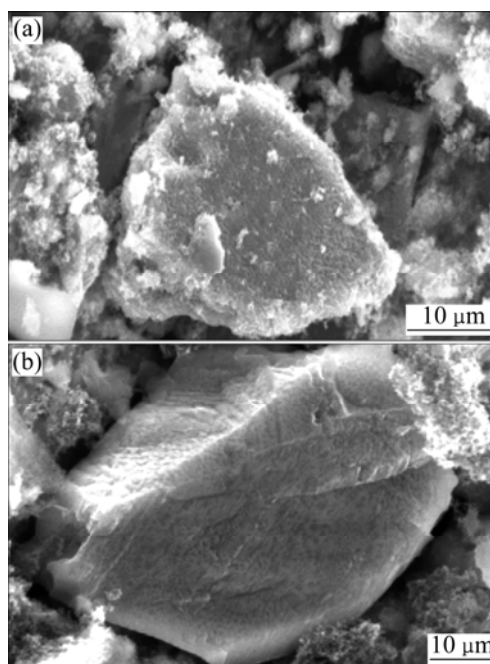
Compared Table 4 with Table 5, it can be seen that the amount of ferrous and zinc ions and the output electric quantity in BEGL process are larger than those in EGL process. After 24 h in BEGL process, the ratio of  $Q_b$  is 22.55%, which shows that the bacterial oxidation on the surface of sphalerite has initiated. Subsequently, the increase in the ratio of  $Q_b$  with the increase of time is up to 27.90% in 72 h. The dissolved rate of  $Zn^{2+}$  in the presence of *A. thiooxidans* is 43% higher than that in the absence of *A. thiooxidans*; the electrogenerative quantity in the former is about 150% more than that in the latter.

The SEM images of the remnant in BEGL and EGL are shown in Fig.3. It can be seen that a large quantity of sulfur floccules is adhere to the surface of unreacted sulfide in EGL process, while the surface of unreacted sulfide in BEGL process is clear. It is concluded that the produced sulfur is partly oxidized in BEGL process compared with EGL process.

## 4 Conclusions

1) The galvanic current for the sphalerite electrode in EGL and BEGL processes predominates over its self-corrosion process.

2) The leaching ratio and the electric quantity output in BEGL process are larger than those in EGL process, and the ratio of biologic electric quantity is as high as 27.90% for 72 h in BEGL process. The dissolved ratio of  $Zn^{2+}$  in the presence of *A. thiooxidans* is nearly 72.16% and 43% more than that that in the absence of *A. thiooxidans*. The electro-generative quantity in the former is about 150 % more than that in the latter.

**Fig.3** SEM images of oxidation debris of sphalerite: (a) EGL process; (b) BEGL process

3) The first stage in EGL and BEGL processes is the dissolution of sphalerite on the surface to ions and sulfur element, which is oxidized by oxygen in promotion of *A. thiooxidans* in the further procedure in the latter.

## References

- [1] WANG S F, FANG Z, WANG Y, CHEN Y. Electrogenative leaching of galena with ferric chloride [J]. Minerals Engineering, 2003, 16(2): 869–872.
- [2] WANG Shao-fen, FANG Zheng. Simultaneous electrogenerative leaching of chalcopyrite concentrate and  $MnO_2$  [J]. J Cent South Univ Technol, 2006, 13(1): 49–52.
- [3] WANG Shao-fen, FANG Zheng. Mechanism of the influence of ferric ion on electrogenerative leaching of sulfide minerals with  $FeCl_3$  [J]. Transactions of Nonferrous Metals Society of China, 2006, 16(2): 473–476.
- [4] WANG S F, FANG Z, TAN Y F. Application of thermo-electrochemistry to simultaneous leaching of sphalerite and  $MnO_2$  [J]. Journal of Thermal Analysis and Calorimetry, 2006, 85(3): 741–743.
- [5] WANG S F, FANG Z, TAN Y F. Electrogenative-leaching of mechanically activated galena [J]. Journal of Thermal Analysis and Calorimetry, 2006, 85(3): 745–747.
- [6] WANG S F, XIAO Li, LI Y Q, FANG Z, QIU G Z, LI J. Electrogenative leaching for sphalerite- $MnO_2$  in the presence of *Acidithiobacillus ferrooxidans* [J]. Journal of Thermal Analysis and Calorimetry, 2009, 95(1): 869–872.
- [7] XIAO Li, QIU Guan-zhou, FANG Zheng, LIU Jian-she. Dynamics in simultaneous electro-generative leaching for sphalerite- $MnO_2$  [J]. Transactions of Nonferrous Metals Society of China, 2007, 17(5): 1045–1051.
- [8] XIAO Li, FANG Zheng, QIU Guan-zhou, LIU Jian-she. Electro-generative mechanism for simultaneous leaching of pyrite and  $MnO_2$  in presence of *A. ferrooxidans* [J]. Transactions of Nonferrous Metals Society of China, 2007, 17(6): 1373–1378.

- [9] RAMACHANDRA R S, HEPLER L G. Equilibrium constants and thermodynamics of ionization of aqueous hydrogen sulfide [J]. *Hydrometallurgy*, 1977, 2(2): 293–299.
- [10] DALEWSKI I F. Removing arsenic from copper smelter gases [J]. *JOM*, 1999, 51(1): 24–26.
- [11] XIAO Li, LIU Jian-she, FANG Zheng, QIU Guan-zhou. Factors affecting output power in electro-generative leaching system of Chalcopyrite [J]. *The Chinese Journal of Process Engineering*, 2006, 6(4): 576–579. (in Chinese)
- [12] DEVI N B, MADHUCHHANDA M, SRINIVASA RAO K, PATH P C, PARAMGURU R K. Oxidation of chalcopyrite in the presence of manganese dioxide in hydrochloric acid medium [J]. *Hydrometallurgy*, 2000, 57(1): 57–76.
- [13] HAVLIKA T, LAUBERTOVAA M, MISKUFOVAA A, KONDASB J, VRANKAC F. Extraction of copper, zinc, nickel and cobalt in acid oxidative leaching of chalcopyrite at the presence of deep-sea manganese nodules as oxidant [J]. *Hydrometallurgy*, 2005, 77(1/2): 51–59.
- [14] GANTAYAT B P, RATH P C, PARAMGURU R K, RAO S B. Galvanic interaction between chalcopyrite and manganese dioxide in sulfuric acid medium [J]. *Metallurgical and Materials Transactions B*, 2000, 31(1): 55–61.
- [15] TAKAMI K, SUENAGA Y I, MIGITA A, TAKAHASHI T. Kinetic model for simultaneous leaching of zinc sulfide and manganese dioxide in the presence of iron-oxidizing bacteria [J]. *Chemical Engineering Science*, 2000, 55(17): 3429–3436.
- [16] SANTHIYA D, SUBRAMANLAN S, NATARAJAN K A. Surface chemical studies on galena and sphalerite in the presence of *Thiobacillus thiooxidans* with reference to mineral beneficiation [J]. *Minerals Engineering*, 2000, 13(7): 747–763.

(Edited by ZHAO Jun)